Pol. J. Environ. Stud. Vol. XX, No. X (XXXX), 1-14
DOI: 10.15244/pjoes/220226 ONLINE PUBLICATION DATE: 2026-08-13

Original Research

Characteristics and Prediction of Nitrogen and Phosphorus Loss in Rice Growing Areas of Southern China under Different Irrigation and Drainage Modes

Menghua Xiao[1], Cheng Lu[1], Yu Jin[1], Lei Wang[1], Wanchuan Xiao[1], Dan Xu[1], Ran Xu[1], Yuanyuan Li[2]*

[1]Zhejiang Institute of Hydraulics and Estuary (Zhejiang Institute of Marine Planning and Design), Hangzhou 310020, China
[2]North China University of Water Resources and Electric Power, Zhengzhou 450045, China

Received: 11 December 2025
Accepted: 31 March 2026

Abstract

This study simulates and predicts nitrogen (N) and phosphorus (P) losses in paddy fields under different irrigation modes and rice varieties in the rice-growing regions of southern China. A field experiment was conducted with two rice varieties (Xiushui and Yongyou) and four irrigation modes: conventional flooding (W0), shallow rain-catching irrigation (W1), improved shallow rain-catching irrigation (W2), and furrow-basin rainfall-adapted irrigation (W3). A model integrating water balance and nutrient concentration dynamics was developed to simulate drainage volume and N/P losses, with parameters calibrated and validated using field-measured data. Results showed that irrigation mode significantly influenced N and P losses. The W0 mode exhibited the highest losses, with total nitrogen (TN) and total phosphorus (TP) losses reaching 8.52 kg $N \cdot hm^{-2}$ and 0.72 kg $P \cdot hm^{-2}$, respectively. In contrast, the W3 mode reduced TN and TP losses by approximately 39% and 43%, respectively. The exponential decay-based concentration model demonstrated strong performance, with determination coefficients (R^2) of 0.68 for TN and 0.62 for TP. Spatial analysis identified eastern Xucun Town and northern Huangwan Town as critical source areas for N and P losses. The total estimated TN and TP losses across the irrigation district were 21.43 tons and 3.69 tons, respectively, with loss coefficients ranging between 0.85%-3.32% for TN and 0.49%-1.37% for TP. The study concludes that optimized irrigation practices, particularly W3, effectively mitigate nutrient losses while maintaining crop water requirements. The proposed model offers a reliable tool for simulating and predicting non-point source pollution in paddy systems, supporting the development of targeted pollution control strategies in agricultural watersheds.

Keywords: paddy fields, irrigation modes, nitrogen and phosphorus loss, model simulation, water balance

*e-mail: liya66720@126.com
0000-0001-9061-6885

Introduction

As a staple food for the global population, rice is vital to national economies and livelihoods. In China, ensuring high yields has historically depended on heavy fertilizer use and continuous flooding irrigation. However, this extensive "high-input, high-output" approach has created serious environmental issues, most notably agricultural non-point source pollution from nitrogen (N) and phosphorus (P) loss [1, 2]. Paddy fields act as unique "source-sink" interfaces. Under flooded conditions, N is lost via ammonia volatilization, nitrification-denitrification, runoff, and leaching, while P mainly enters water bodies through runoff and leaching [3, 4]. These lost nutrients are key drivers of eutrophication in rivers, lakes, and reservoirs, causing algal blooms, contaminating drinking water, and elevating nitrate levels in groundwater [5]. Thus, balancing high rice yield with environmental protection for sustainable agricultural development is a critical scientific challenge for China and the world.

Irrigation and drainage management is globally recognized as a key factor in regulating N and P losses from paddy fields. In recent decades, countries such as Japan and the United States have promoted water-saving irrigation techniques, including intermittent and moist irrigation. Compared to traditional continuous flooding, these methods significantly reduce ponding water depth and consequently lower the risk of N and P runoff losses. Moreover, they influence soil nitrogen transformation and leaching by altering soil wetting-drying cycles [6-8]. Research from the University of California has confirmed that intermittent irrigation effectively reduces nitrate leaching into groundwater. China has also made substantial progress in this area. Irrigation regimes such as "thin-shallow-wet-dry", controlled irrigation, rainwater storage irrigation, and furrow irrigation have proven effective in conserving water and reducing N and P losses [9-11]. Studies indicate that compared to continuous flooding, water-saving irrigation practices like intermittent and rainwater-storage irrigation reduce drainage volumes and enhance evapotranspiration, thereby improving water use efficiency. Average total nitrogen (TN) and total phosphorus (TP) runoff losses under continuous flooding were 16.51% and 20.53% higher than under shallow-wet irrigation, and 81.07% and 72.90% higher than under controlled irrigation, respectively. Similarly, TN and TP leaching losses were greater under continuous flooding than under water-saving alternatives. Intermittent irrigation reduced N and P losses by approximately 22.99% and 10.01%, respectively, compared to traditional irrigation, with a corresponding 1% reduction in nitrogen fertilizer loss. When combined with appropriate fertilization and topdressing methods, water-saving irrigation can enhance rice water productivity and nitrogen use efficiency while sustaining high yields [12-14].

Historically, traditional agricultural drainage systems were designed primarily to meet crop water and aeration requirements and, in arid and semi-arid regions, to maintain soil salinity balance. Environmental concerns and the utilization of rainwater were rarely considered. However, surface runoff and subsurface drainage (leaching) represent the primary pathways for N and P losses from paddy fields to water bodies. As a result, minimizing such losses while meeting drainage needs has become a critical research priority. This has spurred interest in controlled drainage strategies. Numerous studies have shown that well-managed controlled drainage can effectively mitigate agricultural non-point source pollution and, under certain conditions, reduce irrigation demand. For instance, combining controlled drainage with shallow irrigation and deep water storage has been found to better regulate field drainage, reduce N and P losses, and improve nutrient use efficiency [15]. Despite these advances, most existing research focuses on the environmental effects of individual irrigation or drainage regimes. Systematic comparisons of N and P loss fluxes, forms, and pathways under different modes (e.g., conventional flooding, intermittent irrigation, plastic film mulching with dry cultivation) remain insufficient.

Accurate prediction is essential for effective risk management. Internationally, mechanistic and semi-mechanistic models – such as DNDC, ORYZA, SWAT, and HYDRUS – have been developed to simulate water cycles in agricultural ecosystems to some extent [16, 17]. Although these models perform well at the macro-watershed scale, challenges remain in accurately simulating specific combinations of crop varieties and management practices at the field scale. In this context, the present research holds significant theoretical value and practical relevance. By investigating the patterns of N and P loss through surface and subsurface pathways under the combined influence of different rice varieties and irrigation-drainage regimes, this study aims to provide technical pathways for precise prevention and control of non-point source pollution. Specifically, it seeks to clarify the characteristics of N and P loss under various "variety-irrigation" combinations, explore the migration pathways and pollution formation mechanisms at the irrigation district scale, and enable the prediction of N and P discharge loads. The findings are expected to play a vital role in optimizing water and nitrogen management in irrigation districts, improving water environment quality, and enhancing the capacity of farmland water infrastructure to adapt to climate change.

Materials and Methods

Experimental Site

The experiment was conducted from 2024 to 2025 at the Pinghu Key Irrigation Experiment Station in Zhejiang Province (121°10'E, 30°43'N). The station is located in the Hangjiahu Plain region, representative of the fundamental water use and environmental characteristics of the grain production area in northern Zhejiang. It covers an area of approximately 3.33 hectares, featuring flat terrain, comprehensive water conservancy infrastructure, and a relatively high groundwater table that generally remains at 0.2-0.5 m below the field surface during the rice growing season.

The soil texture is silty clay, formed from marine sedimentary parent material, with a bulk density of 1.3-1.4 g/cm³. The entire experimental area utilizes pipeline irrigation with water meters for measurement, sourcing irrigation water from the nearby river network.

Experimental Design

This study selected two single-cropping rice varieties – Xiushui (conventional, denoted as X) and Yongyou (hybrid, denoted as Y), combined with four irrigation management modes. These modes are: (1) Conventional Irrigation (W0): Based on local common practices. (2) Shallow Rain-Catching Irrigation (W1): Derived from recent regional applicability research on water-saving irrigation models conducted by the irrigation experiment station network. (3) Improved Shallow Rain-Catching Irrigation (W2): A modified approach based on experimental results from recent years, which refines the original shallow rain-catching irrigation mode. (4) Furrow-Basin Rainfall-Adapted Irrigation (W3): Adopted the rainfall-adapted irrigation technology proposed by the Provincial Water Resources Research Institute of Zhejiang. Specific water control criteria are detailed in Table 1. Consequently, a total of eight treatments were designed (2 varieties × 4 irrigation modes) with 3 replicates each, resulting in 24 experimental plots. Fertilization for all treatments followed the levels recommended by the Soil Testing and Formula Fertilization Project Team of the Zhejiang Academy of Agricultural Sciences. The average application rates were 225 kg/ha of pure nitrogen (N), 100 kg/ha of P_2O_5, and 120 kg/ha of K_2O, applied in three fertilizations throughout the rice growth period.

Indicators and Measurements

i) Meteorological observation: Parameters (including daily mean temperature, daily maximum temperature, daily minimum temperature, air relative humidity, wind speed, wind direction, rainfall, sunshine duration, atmospheric pressure, and evaporation) were observed by an existing automatic weather station (ZQZ-CII).

ii) Rice water consumption: Water consumption was measured by the change in water level in the field surface according to the measuring needle when there was a water layer at 8:00 am every day; when there was no water layer, it was measured by soil water content change according to the soil moisture analyzer every 3-5 days. Water leakage was measured by the leakage meter every day, and then the leakage amount was calculated according to the reading difference by the measuring needle before and after. The transpiration was the difference between water consumption and leakage.

iii) Irrigation and drainage water sampling: Water sample analysis: All samples were sent to a central laboratory for unified testing. The analyzed indicators included TN, TP, COD (Chemical oxygen demand), NO_3^--N (Nitrate nitrogen), and NH_4^+-N (Ammonium nitrogen).

1) Irrigation water sample: If irrigation occurred during any growth stage, a representative sample was collected from the irrigation water source.

2) Drainage water sample: Samples were collected during every drainage event. Sample bottles were labeled with the plot number and growth stage.

3) Seepage water sample: During each growth stage, soil seepage solution was collected once using the paddy field lysimeters.

Table 1. Field water control criteria for different irrigation treatments (Year 2024-2025).

Mode	Lower-upper limit	Re-greening	Tillering		Jointing-booting	Heading-flowering	Milkying	Yellow ripening
			Early	Late				
W0	Lower limit	20	20	30	30	10	10	0
	Upper limit	30(50)	50(70)	60(90)	60(100)	50(100)	50(60)	0(20)
W1	Lower limit	5	$0.8\ \theta_s$	$0.7\ \theta_s$	$0.9\ \theta_s$	0	$0.8\ \theta_s$	Natural drainage
	Upper limit	30(40)	20(50)	20(0)	30(60)	30(60)	20(30)	
W2	Lower limit	5	$0.8\ \theta_s$	$0.7\ \theta_s$	$0.9\ \theta_s$	0	$0.8\ \theta_s$	
	Upper limit	30(50)	20(80)	20(0)	30(140)	30(120)	20(80)	
W3	Lower limit	0	$0.8\ \theta_s$	$0.7\ \theta_s$	$0.8\ \theta_s$	$0.8\ \theta_s$	$0.8\ \theta_s$	
	Upper limit	20(50)	0(100)	0(150)	0(200)	0(300)	0(150)	Natural drainage(50)

Notes: (1) The first number in the upper limit is the storage depth of irrigation water in mm, and the second number in parentheses is the storage depth of rainfall in mm in the paddy field. The lower limit means the field needs irrigation when the soil moisture or water storage depth of the field reaches this level. (2) θ_s is the field water holding capacity in %.

Modeling Nitrogen And Phosphorus Loss

The amount of non-point source nitrogen and phosphorus loss from farmland depends on the drainage volume and the concentrations of nitrogen and phosphorus in the drainage water. This study constructs models for paddy field drainage volume and for nitrogen and phosphorus concentrations in drainage water based on water balance and soil physicochemical adsorption theories to estimate the loss of nitrogen and phosphorus from farmland and their loss coefficients. The drainage volume is calculated using the water balance equation. The concentrations of nitrogen and phosphorus in farmland drainage are simulated by developing models that relate fertilizer application rates, the timing of drainage events, and the equilibrium concentrations of nitrogen and phosphorus in the soil.

Generally, runoff and leaching are the primary pathways for nutrient loss from farmland. In the plains of southern China, precipitation is the main driving force behind agricultural non-point source pollution, primarily entering water bodies through surface runoff and subsurface seepage. Therefore, the following model is constructed to calculate the regional loss of nitrogen and phosphorus from farmland:

$$L = 0.001(\sum_{i=1}^{n} A_i \times R \times C) \quad (1)$$

In the equation, L is the total nitrogen and phosphorus loss from regional farmland (kg); A_i is the irrigated area of cultivation type i (hm^2); R is the drainage volume ($m^3 \cdot hm^{-2}$); C is the nitrogen and phosphorus concentration in the drainage water ($mg \cdot L^{-1}$); 0.001 is the dimensional conversion coefficient.

i) Calculation of drainage volume

Since paddy fields are mostly saturated with soil moisture, have high groundwater levels, and experience minimal changes in soil moisture, the water balance only considers field surface evaporation and crop transpiration (combined as evapotranspiration, ET), irrigation, and rainfall. The drainage volume is calculated using the following equation:

$$R = P + I - ET \quad (2)$$

In the equation, P is precipitation (mm); I is irrigation volume (mm); ET is evapotranspiration (mm).

ii) Simulation of nitrogen and phosphorus concentrations

The concentrations of nitrogen and phosphorus in drainage water are related to fertilizer application rates, the timing of drainage events, and the equilibrium concentrations in the soil. During the initial stage of fertilization, the concentrations of nitrogen and phosphorus in the soil are at their highest level. However, the soil adsorption of nitrogen and phosphorus is also the fastest at this stage, and the transformation processes of nitrogen and phosphorus occur most rapidly. As the soil adsorption capacity increases, the adsorption rate gradually declines, and both the transformation and adsorption processes of nitrogen and phosphorus slow down, eventually reaching an equilibrium state. The entire process can be simulated using a power exponential decay function:

$$C = a_1 F \times exp(-d_1 t) + c_1 \quad (3)$$

In the equation, C is the concentration of drainage ($mg \cdot L^{-1}$); F is fertilizer amount ($kg \cdot hm^{-2}$); a_1 and d_1 are parameters; t is the number of days between the drainage event and irrigation (d); c_1 is the equilibrium concentration ($mg \cdot L^{-1}$).

The parameters a_1, c_1, and d_1 in the above model are influenced by management practices, soil properties, and land use. As a result, the model reflects the integrated effects of agricultural management (such as fertilization and irrigation), rainfall, soil conditions, and other factors. It is characterized by its limited number of parameters and clear physical mechanisms. After parameter calibration, the model can be applied to estimate nitrogen and phosphorus losses from farmland in irrigation districts.

Results

Pollutant Discharge from Field Plots

Pollutant Discharge in Surface Water

Surface water pollution from paddy fields is mainly caused by fertilizers and harmful materials in field drainage, with drainage falling into two categories: proactive drainage for water level management during rice growth, and passive drainage triggered by rainfall. Both pathways carry pollutants such as nitrogen (N) and phosphorus (P) into water bodies. Additionally, a portion of pollutants leaches through the paddy field, contributing to agricultural non-point source pollution.

During the entire rice growth period, drainage was implemented three times (once at the tillering stage and twice at the jointing-booting stage). The specific performance was as follows: W0 drained 105.9 mm, W1 drained 116.9 mm, while both W2 and W3 recorded 0 mm of drainage. This clearly demonstrates that both W2 and W3 achieved zero drainage from the paddy fields. As can be seen from Fig. 1, N and P loads in the surface drainage were dominated by N, with P accounting for a relatively lower proportion. Within the nitrogen load, the NH_4^+-N load was lower than the NO_3^--N load. The overall loads of TP, TN, NO_3^--N, NH_4^+-N, and COD generally followed the trend: W0>W1>W2 ≈ W3. Compared to W0, the W1 mode reduced the loads of TP, TN, NO_3^--N, NH_4^+-N, and COD by 3.7%, 45.9%, 34.0%, 36.1%, and 19.3%, respectively. Analysis incorporating drainage volume indicates that

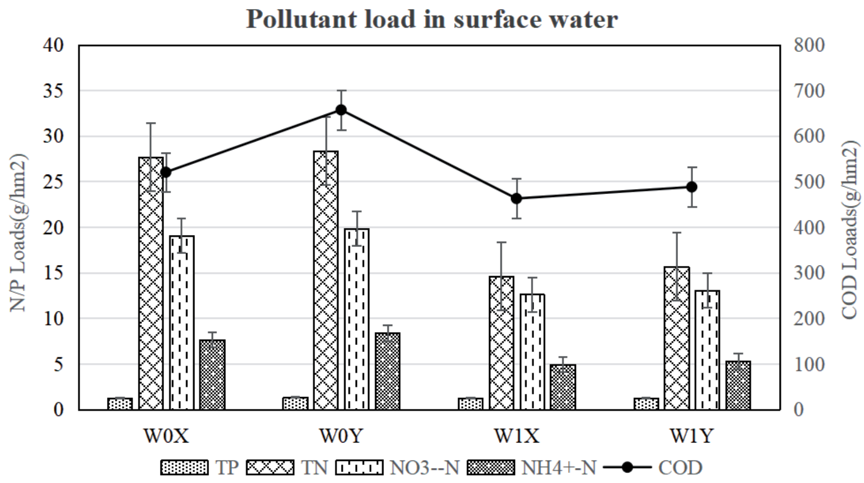

Fig. 1. Pollutant discharge in surface water with different treatments.

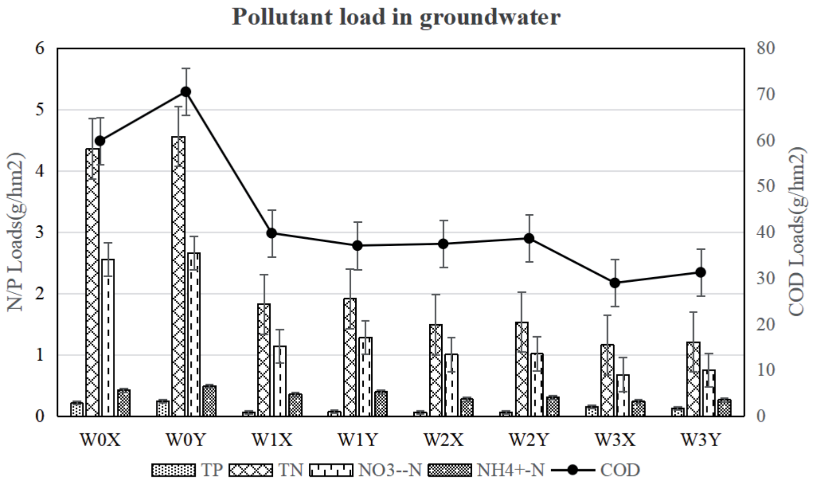

Fig. 2. Pollutant discharge in groundwater with different treatments.

the increase in pollutant discharge was primarily caused by the increased drainage.

Pollutant Discharge in Groundwater

The loads of TN, TP, COD, NO_3^--N, and NH_4^+-N discharged via subsurface seepage are shown in Fig. 2. It can be seen that N was the dominant pollutant in the seepage water, with P accounting for a comparatively lower proportion. Within the nitrogen load, the NH_4^+-N load was lower than that of NO_3^--N. The overall loads of TP, TN, NO_3^--N, NH_4^+-N, and COD generally followed the order: W0>W1>W2>W3. Specifically, compared to the W0 mode: W1 reduced the loads of TP, TN, NO_3^--N, NH_4^+-N, and COD by 71.9%, 58.1%, 53.5%, 18.0%, and 41.1%, respectively. W2 resulted in reductions of 73.2%, 66.1%, 61.3%, 36.4%, and 41.7%, respectively. W3 led to reductions of 32.3%, 73.5%, 72.6%, 44.8%, and 55.9%, respectively. Given that the seepage volume under W0 was higher than that under water-saving irrigation modes (W1, W2, W3), the primary reason for the reduced N and P pollutant discharge via seepage in the W1, W2, and W3 modes was the decrease in seepage volume itself.

Total Pollutant Load from Field Plots

As shown in Fig. 1 and Fig. 2, under W0 and W1 modes, the pollutant loads in surface water were substantially greater than those in seepage water. In contrast, under the W2 and W3 modes, pollutant discharge was primarily attributed to field seepage. The total pollutant load discharges for each treatment are presented in Table 2. The loads of TP, TN, NO_3^--N, NH_4^+-N, and COD all exhibited the same trend: W0>W1>W2>W3. Specifically, compared to the W0 mode: W1 reduced the loads of TP, TN, NO_3^--N, NH_4^+-N, and COD by 13.7%, 47.6%, 36.5%, 35.1%, and 21.4%, respectively. W2 resulted in reductions of 96.0%, 95.9%, 96.1%, 96.8%, and 94.8%, respectively. W3 led to reductions of 90.6%, 96.4%, 96.8%, 97.0%, and 95.4%, respectively. The discharge loads of N

Table 2. Total pollutant load in the whole growth period with different treatments (g/hm^2).

Treatment	TP	TN	NO_3^--N	NH_4^+-N	COD
W0X	1.469	32.029	21.625	8.066	579.875
W0Y	1.584	32.904	22.498	8.847	727.336
W1X	1.303	16.430	13.746	5.291	502.065
W1Y	1.331	17.586	14.351	5.678	524.798
W2X	0.062	1.491	1.002	0.275	37.373
W2Y	0.059	1.533	1.015	0.303	38.561
W3X	0.157	1.157	0.676	0.237	28.880
W3Y	0.130	1.208	0.750	0.265	31.184
W0	1.527	32.467	22.062	8.456	653.606
W1	1.317	17.009	14.048	5.484	513.431
W2	0.061	1.347	0.860	0.270	34.000
W3	0.143	1.183	0.713	0.251	30.032
X	0.748	12.777	9.262	3.467	287.048
Y	0.776	13.308	9.653	3.773	330.470

and P were strongly correlated with field drainage volume. Analysis of the contributions of drainage and seepage to the emission of various non-point source pollutants from the paddy field revealed that approximately 88.0%, 84.9%, 87.4%, 92.3%, and 88.6% of the TP, TN, NO_3^--N, NH_4^+-N, and COD loads, respectively, originated from surface drainage. Therefore, the majority of non-point source pollutant discharge from this field plot came from surface drainage, with minimal variation observed between different rice varieties.

Determination of Parameters for the Field-Scale Nitrogen and Phosphorus Loss Model

Parameter Acquisition of the Model

Rice has high water requirements during its early and middle growth stages, thus substantial irrigation throughout its entire growth cycle is necessary to support normal development. During the growth period, the total amount of irrigation and rainfall in the paddy field exceeds the crop water requirement, leading to drainage following irrigation events. The irrigation volumes, effective rainfall, and rice water consumption for each treatment are presented in Table 3.

Parameter Acquisition for Model Uncertainty Analysis

The Monte Carlo method was employed to analyze model uncertainty. As a common approach for model uncertainty analysis, Monte Carlo simulation translates parameter uncertainty into uncertainty in the model outputs. Based on statistical analysis of existing data, this study assumed that the drainage volume per irrigation event (R) follows a uniform distribution, while the nitrogen and phosphorus concentrations in drainage water (C) follow a standard normal distribution. Using Excel, 400 random numbers were generated for each parameter according to their respective distributions to serve as parameter samples. The uncertainty range of the calculated results from the crop nitrogen and phosphorus loss model was then analyzed, with the outcomes presented in Table 4.

Parameter Calibration and Validation

Based on the measured water quality data from drainage samples across all treatment groups, the key parameters (a_1, d_1, and c_1) of the nitrogen and phosphorus concentration variation function in the model were calibrated. The results are presented in Fig. 3. Using drainage time as the independent variable, the model was fitted to the trends of TN and TP concentrations in the drainage water samples. A nonlinear exponential decay function was employed to represent the decreasing characteristic of nutrient concentrations.

For TN, the fitted parameters were $a_1 = 3.74$, $d_1 = 0.22$, and $c_1 = 0.45$, with a coefficient of determination (R^2) of 0.68. This indicates that the model effectively explains the decreasing process of TN concentration over time during drainage. For TP, the parameters were $a_1 = 0.76$, $d_1 = 0.22$, and $c_1 = 0.05$, with an R^2 of 0.62, also demonstrating a good fit.

Furthermore, the linear correlation between the model-fitted values and measured values further verified the reliability of the model (TN: $y = 0.823x + 0.207$,

Table 3. Summary of water balance components during the rice growing stage (mm).

Treatment	Irrigation volume	Effective rainfall	Percolation		Evapotranspiration		Water Consumption	
			Total	Daily average	Total	Daily average	Total	Daily average
W0X	353.3	190.4	51.6	0.44	491.4	4.20	543.0	4.64
W0Y	367.4	190.4	56.8	0.49	514.3	4.40	571.1	4.88
W1X	272.2	114.0	24.5	0.21	361.9	3.09	386.4	3.30
W1Y	297.8	118.9	28.9	0.25	383.0	3.27	411.9	3.52
W2X	147.6	322.3	29.3	0.25	441.0	3.77	470.3	4.02
W2Y	148.4	327.3	33.6	0.29	452.1	3.86	485.7	4.15
W3X	175.9	344.9	31.2	0.27	489.8	4.19	521.0	4.45
W3Y	149.7	364.8	27.8	0.24	490.0	4.19	517.8	4.43

Table 4. Parameter ranges for Monte Carlo simulation.

Treatment	Drainage volume per irrigation event ($m^3 \cdot hm^{-2}$)		TN concentration ($mgN \cdot L^{-1}$)		TP concentration ($mg \cdot L^{-1}$)	
	Range	Mean (Standard deviation)	Range	Mean (Standard deviation)	Range	Mean (Standard deviation)
W0X	680–990	885.7(±228.4)	0-5.21	4.18(±0.98)	0-0.46	0.35(±0.07)
W0Y	720–1006	912.6(±227.1)	0-4.92	4.03(±0.76)	0-0.43	0.34(±0.09)
W1X	660–940	735.2(±194.5)	0-4.62	3.96(±0.88)	0-0.38	0.31(±0.08)
W1Y	670–950	748.9(±206.0)	0-4.40	3.77(±0.97)	0-0.37	0.28(±0.07)
W2X	240–530	398.3(±27.7)	0-4.23	3.45(±0.72)	0-0.33	0.27(±0.08)
W2Y	250–575	423.1(±25.8)	0-4.02	3.29(±0.65)	0-0.35	0.24(±0.05)
W3X	230–320	287.5(±26.3)	0-3.86	2.98(±0.55)	0-0.31	0.24(±0.03)
W3Y	235–310	280.7(±21.9)	0-3.61	2.89(±0.66)	0-0.29	0.23(±0.03)

$R^2 = 0.68$; TP: $y = 1.090x + 0.125$, $R^2 = 0.62$). The results show that the constructed exponential model achieves high accuracy in describing the dynamics of nitrogen and phosphorus concentrations in paddy field drainage within the irrigation district. It can serve as an effective tool for simulating nitrogen and phosphorus losses and estimating loads at the watershed scale.

Simulation of Drainage Volume and Nitrogen-Phosphorus Loss

Model Validation

Using the data obtained from the water quality monitoring point, the simulation results of drainage volume and nitrogen-phosphorus loss were validated. The model validation results are shown in Fig. 4. The simulated drainage volume was 320 $m^3 \cdot hm^{-2}$, while the measured value was 340 $m^3 \cdot hm^{-2}$, with an error of 6%. The simulated TN loss was 1.40 kg $N \cdot hm^{-2}$, while the measured value was 1.55 kg $N \cdot hm^{-2}$, with an error of 10%. The simulated TP loss was 0.115 kg $P \cdot hm^{-2}$, while the measured value was 0.125 kg $P \cdot hm^{-2}$, with an error of 8%. The results indicate that the model can effectively simulate the processes of farmland drainage and nitrogen-phosphorus loss, demonstrating good applicability and reference value.

Loss Amount Simulation and Loss Coefficient Calculation

Based on the field water balance and nitrogen-phosphorus concentration model, this study estimated the total nitrogen (TN) and total phosphorus (TP) loss amounts and their loss coefficients under different irrigation regimes during the rice growth period (Fig. 5). The results indicate that the nitrogen and phosphorus loss loads of each treatment group showed significant differences with adjustments in the irrigation schedule.

In the W0 treatment group (conventional irrigation), the high irrigation frequency and prolonged standing water duration led to the most severe nutrient leaching. The estimated TN losses over the entire rice

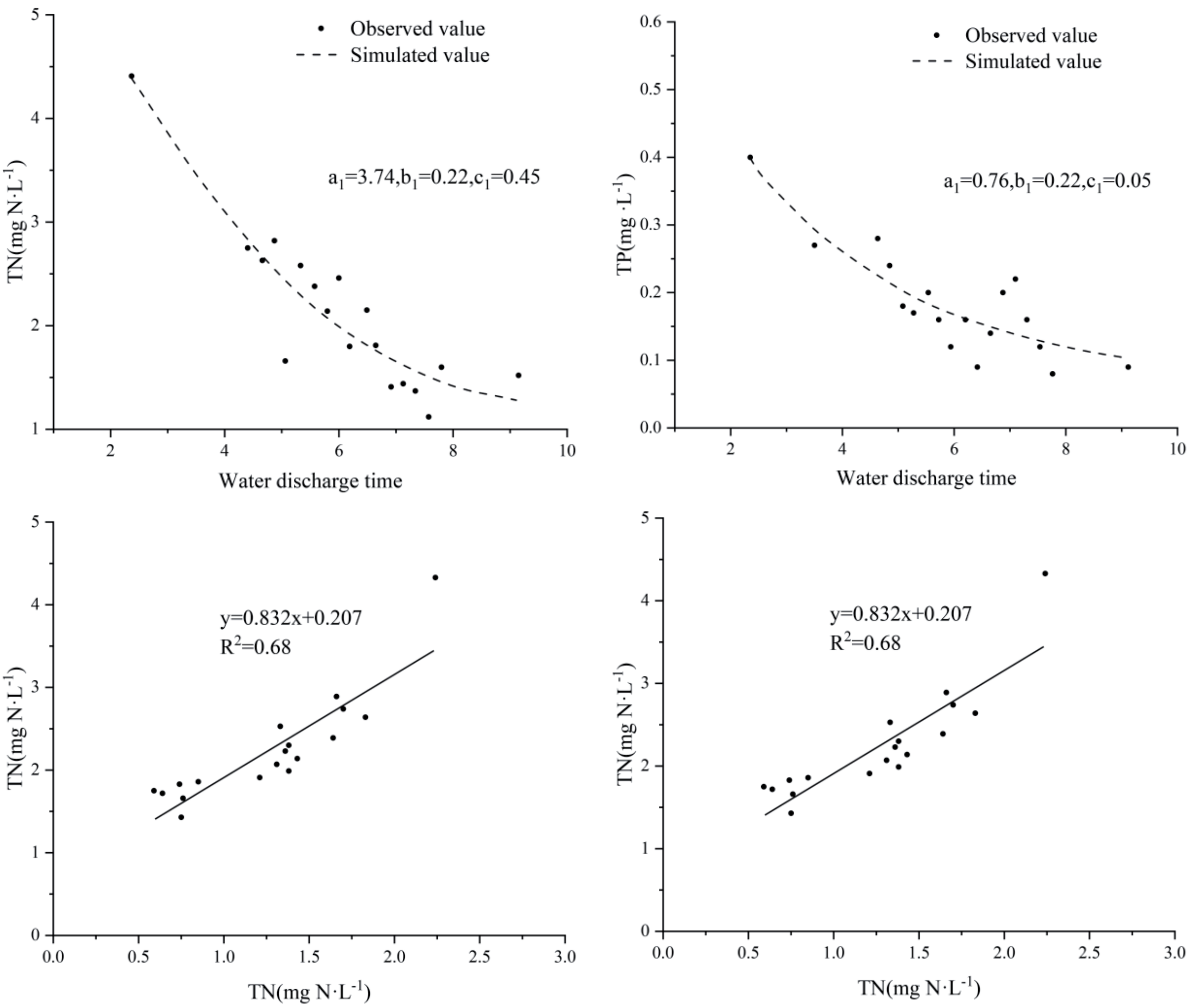

Fig. 3. Calibration of parameters for the model.

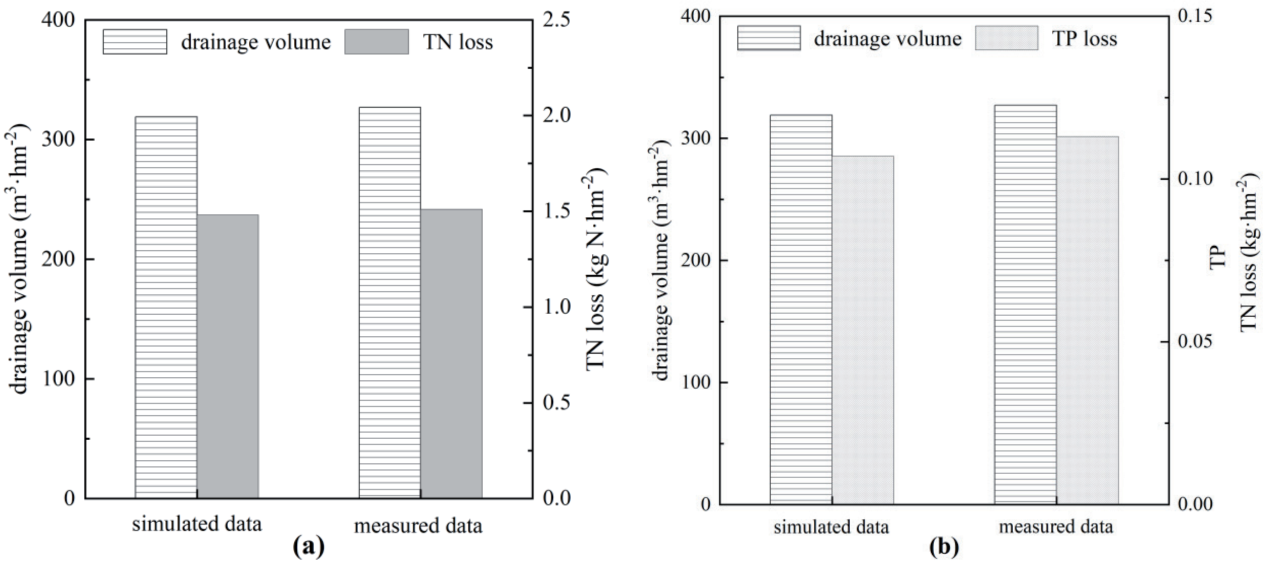

Fig. 4. Validation of simulation results.

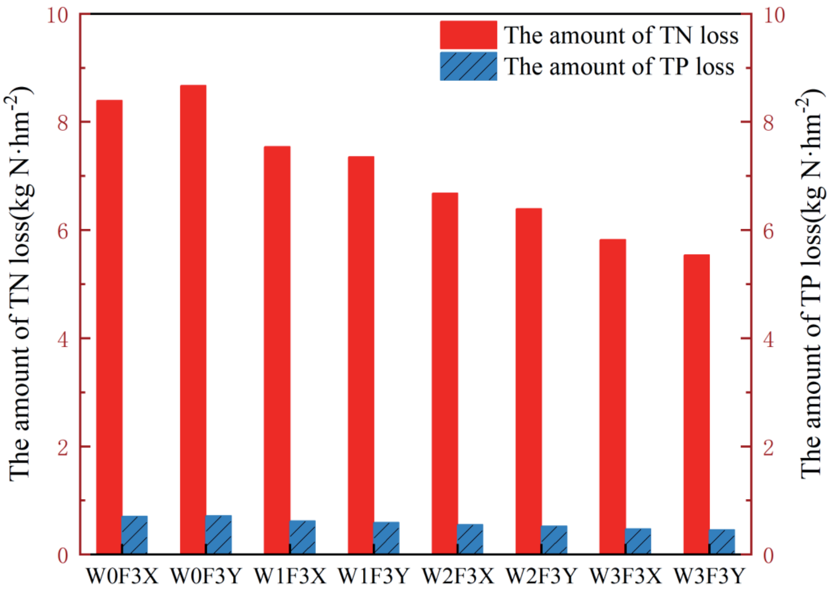

Fig. 5. Temporal variation of nitrogen and phosphorus losses in paddy fields during the rice growth period.

season were 8.22 kg N·hm^{-2} (W0X) and 8.52 kg N·hm^{-2} (W0Y), while TP losses were 0.70 kg P·hm^{-2} and 0.72 kg P·hm^{-2}, respectively. The high irrigation volume and prolonged waterlogging exacerbated nutrient leaching, resulting in the highest nitrogen and phosphorus loss coefficients among all treatments.

In the W1 treatment group (thin-layer intermittent irrigation), nitrogen and phosphorus losses were effectively reduced by decreasing the water depth and shortening the irrigation duration. The TN losses were 7.26 kg N·hm^{-2} (W1X) and 7.08 kg N·hm^{-2} (W1Y), while TP losses were 0.61 kg P·hm^{-2} and 0.58 kg P·hm^{-2}, respectively. This reflects that controlling water layer thickness and irrigation timing can, to some extent, mitigate nutrient loss.

The W2 treatment group (improved rainwater-harvesting thin-layer irrigation) further managed infiltration and runoff processes based on rainwater utilization, demonstrating better water and nutrient regulation. The TN losses were 6.30 kg N·hm^{-2} (W2X) and 6.00 kg N·hm^{-2} (W2Y), while TP losses decreased to 0.53 kg P·hm^{-2} and 0.49 kg P·hm^{-2}, respectively. This indicates that the improved irrigation mode aligns more closely with the goal of coordinated water and nutrient management.

The W3 treatment group (furrow-ridge rainfall-adaptive irrigation) performed the best, achieving minimal nutrient loss through on-demand water supply and decentralized drainage regulation. The TN losses decreased to 5.34 kg N·hm^{-2} (W3X) and 5.04 kg N·hm^{-2} (W3Y), while TP losses were the lowest, at only 0.43 kg P·hm^{-2} and 0.41 kg P·hm^{-2}, respectively. This demonstrates that this irrigation mode significantly enhances irrigation efficiency and reduces surface runoff and nutrient loss.

Overall, as the irrigation regime was optimized from W0 to W3, nitrogen and phosphorus losses showed a decreasing trend. Compared to conventional irrigation (W0), the TN and TP losses under the W3 treatment were reduced by approximately 39% and 43%, respectively, indicating that refined irrigation regulation significantly contributes to mitigating agricultural non-point source pollution and improving water and nutrient use efficiency. These results provide a scientific basis for efficient water use and ecological protection in rice irrigation areas.

Model Uncertainty Analysis

In this study, the field-scale nitrogen and phosphorus loss model integrates the water balance and concentration evolution processes. Although the overall fitting accuracy is high, the model results still exhibit certain uncertainties, primarily reflected in the following aspects:

i) Input data error: The fundamental data relied upon by the model, such as rainfall, irrigation, and evapotranspiration, are sourced from monitoring equipment and manual records. Limitations in sensor accuracy, deployment spacing, and human operation may introduce systematic errors, thereby affecting the accuracy of drainage volume simulations.

ii) Concentration model parameter sensitivity: The temporal variation of nitrogen and phosphorus concentrations is fitted using a power-exponential function. Its key parameters (e.g., initial concentration coefficients a_1, d_1, c_1) are obtained through regression fitting. While the overall correlation is good, there is a risk of local overfitting or low explanatory power under specific treatments, leading to reduced adaptability to extreme weather or abnormal fertilization scenarios.

iii) Model structure simplification: The current model assumes uniform water layer distribution in

Table 5. Paddy field area and nitrogen-phosphorus loss coefficients of townships in the Shangtang River irrigation district.

Town	Paddy field area (hm^2)	TN loss		TP loss	
		Total amount (kg)	Loss coefficients (%)	Total amount (kg)	Loss coefficients (%)
Dingqiao	353.3	1539.80	1.33	265.35	1.12
Huangwan	367.4	2840.99	1.01	489.59	0.97
Xucun	272.2	8096.52	0.85	1395.27	0.49
Yanguan	297.8	703.58	3.32	121.25	1.37
Chang'an	147.6	5631.47	0.89	970.47	0.66
Zhouwangmiao	148.4	2619.46	1.24	451.41	0.57

paddy fields and stable runoff pathways. It does not fully account for heterogeneous factors present in actual irrigation districts, such as topographic relief, connectivity between fields, and differences in farmer irrigation and drainage behaviors. This may lead to underestimation or overestimation of nutrient output risks in local areas.

iv) Impact of external environmental fluctuations: Extreme climate events, such as sudden changes in rainfall intensity, prolonged drought, or high-temperature weather, can disrupt the established relationship between water quantity and quality. The current model lacks a dynamic response mechanism, limiting its predictive capability for abnormal years.

In summary, it is recommended that future research incorporates more observational data to conduct model parameter sensitivity analysis and uncertainty quantification. Methods such as Monte Carlo simulation and Bayesian calibration should be introduced to assess prediction intervals. Furthermore, progressively developing more refined coupled water-fertilizer models is advised to enhance the model's adaptability across different regions and years.

Estimation of Spatial Distribution of Field Nitrogen and Phosphorus Loss

The spatial distribution of TN and TP loss from paddy fields in each administrative unit was simulated by integrating the paddy field area of each township, as shown in Table 5 and Fig. 6. The total TN loss from paddy fields across the entire irrigation district during the rice growing period was 21.43 tons, with specific contributions as follows: Xucun Town (8.09 tons),

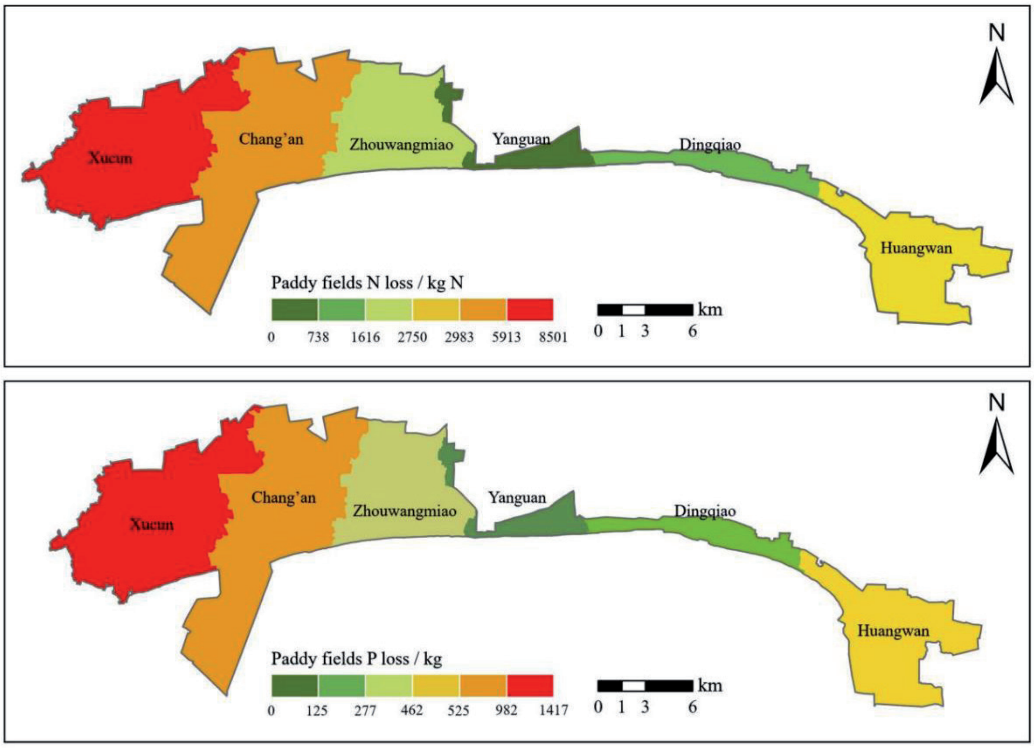

Fig. 6. Nitrogen and phosphorus losses in paddy fields during the rice growth period.

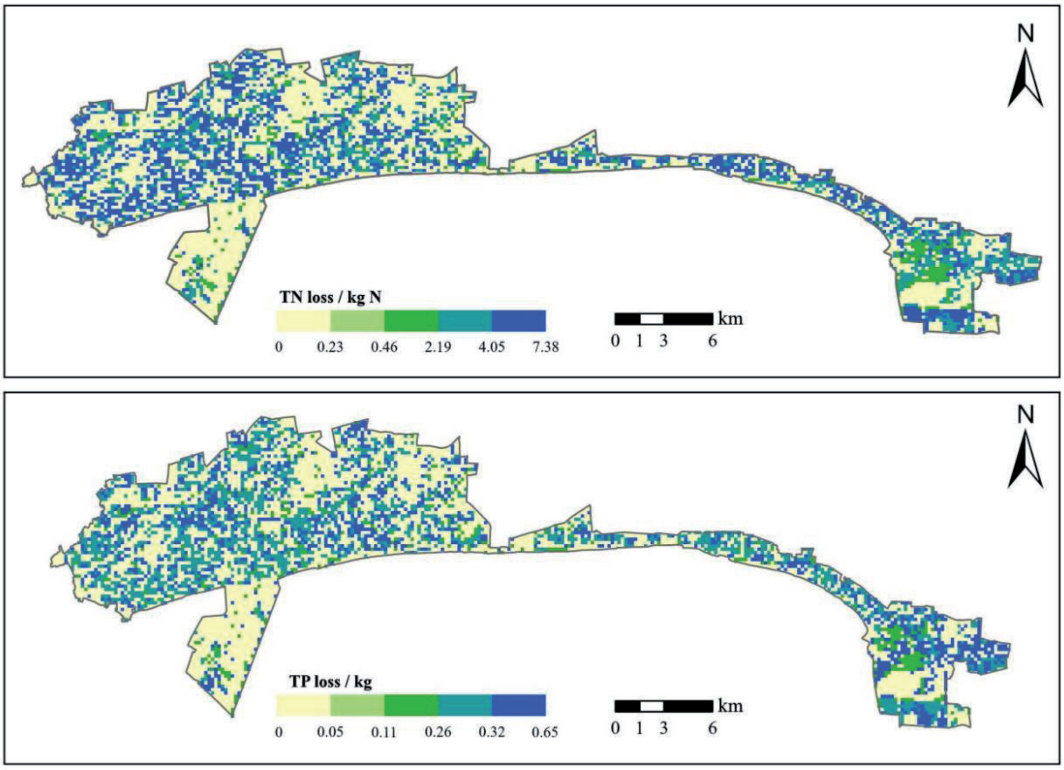

Fig. 7. Spatial pattern of nitrogen and phosphorus loss intensity in farmland of irrigated areas (200 m).

Dingqiao Town (1.54 tons), Huangwan Town (2.84 tons), Chang'an Town (5.63 tons), Zhouwangmiao Town (2.62 tons), and Yanguan Town (0.70 tons). The total TP loss during the entire growing period across the irrigation district was 3.69 tons. The nitrogen and phosphorus loss coefficients ranged from 0.85% to 3.32% and 0.49% to 1.37%, respectively.

Furthermore, the aforementioned nitrogen and phosphorus loss loads from farmland in the irrigation district were allocated to a 200 m × 200 m resolution raster image, resulting in a spatial pattern map of nitrogen and phosphorus loss intensity from farmland in the Yellow River Diversion Irrigation District. As shown in Fig. 7, the spatial patterns of TN and TP loss intensity in the farmland of the irrigation district are generally consistent. The eastern part of Xucun Town, the area connecting with Chang'an Town, and the northern part of Huangwan Town are identified as hotspot areas for nitrogen and phosphorus losses.

Discussion

Emission Reduction Mechanisms and Development Pathways of Water-Saving Irrigation Technologies

Promoting advanced water-saving irrigation models – such as rainwater-storage thin-layer moist irrigation and furrow-basin adaptive rainfall irrigation – represents a key technological pathway for achieving green agricultural development in the rice-growing regions of southern China. A substantial body of research has confirmed that shifting from traditional continuous flooding to water-saving irrigation can generate significant emission reduction benefits in farmland. The underlying mechanisms are primarily reflected in the following three physical pathways. First, direct reduction of drainage volume. Water-saving irrigation methods (e.g., controlled irrigation, intermittent irrigation, thin-layer exposure irrigation) reduce the probability and total volume of surface runoff by lowering the field water level or creating alternating wet-dry conditions. This directly cuts off the main pathway for the loss of dissolved nutrients – such as ammonium nitrogen, nitrate nitrogen, and soluble phosphorus – via water flow [18-20]. Second, reduction of seepage volume. Lower field water pressure reduces the driving force for downward water percolation, thereby decreasing the leaching loss of soluble nutrients like nitrate nitrogen into groundwater [21]. These first two mechanisms align with the findings of this study. Furthermore, water-saving irrigation can alter the soil microenvironment, affecting nutrient transformation and fixation. The alternating wet-dry process strongly influences soil redox potential, thereby regulating nitrogen nitrification and denitrification processes. Although some studies suggest that moderate drying may promote gaseous nitrogen loss through denitrification, the general consensus is that it effectively reduces the liquid-phase export of nitrogen to water bodies. Simultaneously, wet-dry cycles can also enhance soil adsorption and fixation of phosphorus, reducing its activity and migration risk

[22]. Nevertheless, the long-term environmental effects of water-saving irrigation warrant further investigation. For instance, could sustained reduction in seepage volume negatively impact regional groundwater recharge? In drought years, might rainwater-storage practices increase the risk of water stress for rice? Future research should evaluate the comprehensive ecological impacts of these irrigation models over longer time scales and across larger spatial extents.

Genetic Variation and Emission Reduction Potential of Different Rice Varieties

The variation in emission reduction potential among different rice varieties is primarily attributed to genetic differences in key physiological and morphological traits, including root architecture, nutrient uptake efficiency, metabolic processes, and water use efficiency. Studies have shown that rice varieties with well-developed root systems and high nitrogen translocation efficiency can allocate more absorbed nitrogen to grains, exhibiting a high nitrogen harvest index, thereby reducing nitrogen surplus in the farmland system. Certain rice genotypes have been found to enhance nitrogen and phosphorus use efficiency, thereby contributing to the mitigation of agricultural non-point source pollution [23, 24]. Regarding phosphorus utilization, significant genotypic variation also exists in phosphorus uptake efficiency. Some varieties can more efficiently utilize soil and fertilizer phosphorus by secreting organic acids to activate insoluble phosphorus in the soil or by forming more root hairs to increase the absorption surface area. This reduces the risk of phosphorus fixation in the soil and subsequent runoff loss [25, 26]. In the present experiment, the difference in pollutant discharge between the two rice varieties was not statistically significant, which may be attributable to the specific characteristics of the selected varieties or the relatively high fertilizer application level in the trial. Future research should expand the scope of variety screening and systematically investigate the intrinsic relationship between physiological traits – such as root architecture and nutrient uptake kinetics – and nitrogen and phosphorus loss dynamics. Such efforts will provide a theoretical foundation for breeding synergistic rice varieties that integrate water-saving, emission-reducing, and high-yielding traits. In parallel, subsequent studies should focus on optimizing integrated water and fertilizer management schemes, reducing uncertainties in model applications, and conducting multi-scale integrated research. The ultimate goal is to develop a systematic, comprehensive prevention and control technology system for paddy field non-point source pollution, encompassing everything from source reduction to process interception.

Conclusions

This study systematically assessed the characteristics of nitrogen and phosphorus losses under different irrigation patterns in the paddy fields of southern China through field experiments and modeling. A plot-scale predictive model was developed. Key findings are:

(1) Irrigation patterns significantly affect N and P loss pathways and fluxes. Water-saving irrigation, especially improved rainfall-storage shallow intermittent and furrow-rainfall-adapted irrigation, reduced surface runoff to nearly zero and cut total N and P loads by over 90% compared to traditional flooding. Optimizing irrigation for source drainage control is the most effective strategy to mitigate non-point source pollution.

(2) Primary loss pathways vary by irrigation: surface drainage dominates under traditional flooding and shallow intermittent irrigation, while subsurface seepage prevails under improved rainfall-storage and rainfall-adapted irrigation. Differentiated measures balancing "runoff control" and "seepage reduction" are needed.

(3) The developed model, based on water balance and nutrient adsorption theory, reliably simulates drainage volume and N/P concentration dynamics, with errors within an acceptable range. It serves as a practical tool for estimating pollution loads and predicting risks at the irrigation district scale.

(4) Spatial analysis in the Shangtang River irrigation district identified hotspot areas, with total losses of 21.43 t TN and 3.69 t TP during the rice season. High-load zones were located in eastern Xucun Town and adjacent Chang'an Town, providing clear targets for precise zonal control of non-point source pollution.

Acknowledgments

Our research was financially supported by Provincial Research Institute Special Projects of Zhejiang Institute of Hydraulics and Estuary (Zhejiang Institute of Marine Planning and Design) (ZIHEYS25001, ZIHEYS23001), Water Conservancy Science and Technology in Zhejiang Province (RB2410), and Basic Public Welfare Research Project of Zhejiang Province (LGN20E090001, LGN23E090001, LTGN24E090001).

AI Usage Disclosure Statement

Deepseek was used only during the manuscript preparation stage solely for minor linguistic polishing, grammar checking, punctuation correction, and consistency in terminology across the manuscript. All data were collected and analyzed manually by the authors using standard laboratory and statistical methods described in the Methods section. No artificial intelligence tools were involved in any data analysis-related tasks and statistical inference throughout the research. AI-generated outputs were fully reviewed, revised, validated, and approved by the authors.

Conflict of Interest

The authors declare no conflict of interest.

References

1. LIU L.H, OUYANG W., WANG Y., LIAN Z., PAN J., LIU H., CHEN J., NIU S. Paddy water managements for diffuse nitrogen and phosphorus pollution control in China: A comprehensive review and emerging prospects. Agricultural Water Management, **277**, 108102, **2023**.
2. LI S.S., ZHUANG Y.H., LIU H.B., WANG Z., ZHANG F., LV M., ZHAI L., FAN X., NIU S. CHEN J. Enhancing rice production sustainability and resilience via reactivating small water bodies for irrigation and drainage. Nature Communication, **14**, 3794, **2023**.
3. GONG S.F., DING W.H., JU X.H., XIAO N.W., YE Q.S., HUANG J., LI H. Source analysis and control strategies of non-point source pollution in typical agricultural small watershed: A case study of Danjiangkou water conservation area. Scientia Agricultura Sinica, **54** (18), 3919, **2021** [In Chinese].
4. FENG J.Y., ZHANG H., ZHANG J.Y., KANG X.R., WANG H., PAN H., YANG Q., YANG Z., SUN Y., LOU Y. Characteristics of spatial and temporal transport of N and P under coordinated management of ditches and rivers in the plain river network area. Chinese Journal of Eco-Agriculture, **33**, 301, **2025** [In Chinese].
5. FENG J.Y., ZHANG H., ZHANG J.Y., KANG X.R., WANG H., PAN H. Optimization of fertilization combined with water-saving irrigation improves the water and nitrogen utilization efficiency of wheat reduces nitrogen loss in the Nansi Lake basin, China. Journal of Integrative Agriculture, **24** (10), 4034, **2025**.
6. MIN J., SHI W. Nitrogen discharge pathways in vegetable production as non-point sources of pollution and measures to control it. Science of the Total Environment, **613-614**, 123, **2018**.
7. CHEN X., YANG S.H., JIANG Z.W., DING J., SUN X. Biochar as a tool to reduce environmental impacts of nitrogen loss in water-saving irrigation paddy field. Journal of Cleaner Production, **290**, 125811, **2021**.
8. QIU H.N., YANG S.H., JIANG Z.W., XU Y., JIAO X.Y. Effect of irrigation and fertilizer management on rice yield and nitrogen loss: a meta analysis. Plants, **11** (13), 1690, **2022**.
9. LIU L.G., CHEN Y., WU X., YU Q.A., PAN S.B., YANG X.W. Growth characteristics of rice, water-fertilizer utilization and nitrogen and phosphorus loss law under different water-fertilizer control patterns. China Rural Water and Hydropower, **12**, 67, **2020**.
10. HE C. Effects of furrow irrigation on the growth, production and water use efficiency of direct sowing rice. Scientific World Journal, **10**, 1483, **2010**.
11. WANG Y., HU N., CHEN L.H., LIU Q.S., LU Q.L., LI S.W., QIU S.T. Effects of rainfall storage and controlled irrigation mode on phosphorus concentration and water use efficiency of paddy field after tillering fertilizer in Erhai lake basin. Journal of Agro-Environment Science, **45** (3), 702, **2026**.
12. HUA K.J. Mechanisms of water-saving irrigation and slow-release fertilization effects on water-nitrogen transport and transformation in paddy-rice systems. Master Thesis. China Three Gorges University, 24, **2024**.
13. QIN Z.Y. Nitrogen and phosphorus transfer, utilization and stoichiometry in black soil paddy fields under different water and nitrogen management modes. Dongbei Agriculture University, 20, **2022**.
14. ZHANG L.J., MA Y.H., SHI Y.Y., ZHU X.H., WANG L.T., MA Z.Y. Effects of irrigation and fertilization on nitrogen and phosphorus runoff from paddy field. Journal of Soil and Water Conservation, **25**, 7, **2011** [In Chinese].
15. SHAO D.G., QIAO X., LIU H.H., CHAI M.Y., WANG J.Z. Study of moving and transforming law of water and fertilizer under different treatments of irrigation and drainage. Engineering Journal of Wuhan University, **43**, 409, **2010** [In Chinese].
16. RUAN B.N., WU L., GUO J.W., DU B.L. Assessment and selection of the best management practices for the Jinghe River Basin considering the comprehensive benefits of environmental costs. China Environmental Science, **44**, 319, **2024** [In Chinese].
17. LIU L.L., OUYANG W., BAI Y., HAO F.,H. Evaluation on the reduction potential of diffuse nitrogen pollution in paddy field watersheds based on field-ditch-pond system optimization. China Environmental Science, **45**, 2693, **2025** [In Chinese].
18. SHAO P.Y., LI Y.L., XIONG Y.J., YUAN N.N., SU P.L. Reusing effluent water in drainage ditches for irrigation in hilly regions. Journal of Irrigation and Drainage, **42**, 136, **2023**.
19. BELDER P., BOUMAN B.A.M., CABANGON R., GUOAN L., QUILANG E.J.P., LI Y.H., SPIERTZ J.H.J., TUONG T.P. Effect of water-saving irrigation on rice yield and water use in typical lowland conditions in Asia. Agricultural Water Management, **65** (3), 193, **2004**.
20. GAO S.K., YU S.E., WANG M., CAO R.Z., GUO R. Effect of controlled irrigation and drainage on saving water and reducing nitrogen and phosphorus loss in paddy field under alternate drought and flooding condition. Tanslations of the Chinese Society of Agricultural Engineering, **33**, 122, **2017** [In Chinese].
21. XIAO X., ZOU Z.K., CHEN Y.F., LUO W.B., LI Y.L., YANG Z.L. Improving irrigation and fertilization to reduce water usage and nitrogen pollution from rice fields in southern China. Journal of Irrigation and Drainage, **42**, 67, **2023**.
22. ZHANG Z.X., SUN D., LI T.C., QI Z.J., DU S.C., WANG B., HUANG Y. Effects of water-saving irrigation and reducing phosphorus fertilizer on rice yield, phosphorus utilization and soil phosphorus balance in black soil. Tanslations of the Chinese Society of Agricultural Engineering, **38**, 67, **2022**.
23. LIU L.J., WANG K.J., BIAN J.L., XIONG Y.W., CHEN L., WANG Z.Q., YANG J.C. Differences in yield response to nitrogen fertilizer among rice cultivars and their relationship with root morphology and physiology. Acta Agronomica Sinica, **40** (11), 1999, **2014**.
24. ZHANG X.G., XU CM., CHEN S., JI C.L., ZHANG X.F., WANG D.Y. Absorption characteristics of ammonium lon of roots in different nitrogen use efficiency rice varieties. Scientia Agricultura Sinica, **48** (22), 4428, **2015**.

25. LI L., ZHANG X.Z., LI T.X., YU H.Y., LI J., CHEN G.D. Characteristics of phosphorus uptake and use efficiency of rice with high yield and high phosphorus use efficiency. Chinese Journal of Applied Ecology, **25**, 1963, **2014** [In Chinese].

26. WANG X.H., CAO Y.J., WEI W.W., LIU S.L., LV Y.J., LIU C.G., WANG Y.J., WANG L.C. Phosphorus utilization characteristics of forty spring maize hybrids with high-yielding potential in north of China. Journal of Plant Nutrition and Fertilizer, **21**, 580, **2015** [In Chinese].